JOURNAL OF SOLID STATE CHEMISTRY 21, 195–201 (1977)

Lattice Instabilities in $Cs_2MFe(CN)_6$ ($M = Mg^{2+}$, Ca^{2+}, and Sr^{2+}): The Crystal Structure of $Cs_2BaFe(CN)_6 \cdot 2H_2O$

J. J. RAFALKO, B. I. SWANSON AND G. W. BEALL

Department of Chemistry, The University of Texas at Austin, Austin, Texas 78712

Received November 17, 1976; in revised form February 2, 1977

The room temperature Raman spectra of $Cs_2MFe(CN)_6$ ($M = Mg^{2+}$, Ca^{2+}, and Sr^{2+}) suggest that these salts undergo phase transformations similar to those found in $Cs_2LiCr(CN)_6$ where the distortion from the high-symmetry phase proceeds primarily along two modes of vibration. The distortion involves an antiferroelectric rotation of the hexacyanide moiety and a cesium translation. On the basis of the spectra a correlation has been made between the size of M and the apparent transition temperature. In going down the alkaline earths, the apparent transition temperature increases. The structure of the barium salt determined at room temperature shows the crystal latitce contains two waters of hydration. Many similarities have been found between $Cs_2BaFe(CN)_6 \cdot 2H_2O$ and the low-symmetry phase structure of $Cs_2LiCr(CN)_6$.

Introduction

The perovskites have served as the prototypes for describing phase transformations in terms of distortions along particular modes of vibration (*1*). The simplicity of their composition has been partly responsible for the early elucidation of their distortion pathways. Much less is known about phase transformations in crystalline solids containing discrete complex ions. Part of the problem here is the complexity introduced by the additional degrees of freedom of the complex ion itself. Phase transformations for salts containing discrete complex ions may involve distortions along internal modes of vibration as well as lattice modes. However, phase transformations in crystalline solids containing complex ions with strong internal forces present no new difficulties.

The phase transformations of $Cs_2LiCr(CN)_6$ were recently described purely in terms of distortions along lattice modes (*2*). In the high-symmetry $Fm3m$ phase the Li^+ and $Cr(CN)_6^{3-}$ moieties occupy octahedral sites while the Cs^+'s fit loosely into tetrahedral holes defined by the Cr–C–N–Li superstructure (*3*, *4*). The Cs^+'s have abnormally high thermal motions as is consistent with the large distances between the cesium ions and their nearest neighbors. The distance between Cs^+ and the nearest CN^- group is much greater than the sum of the Slater ionic radii for these species. (*5*). This creates a lattice instability which is manifest in structural phase changes where the Cs^+ and CN^- moieties move toward one another. These movements, which correspond to an F_{1u} Cs^+ translation and an F_{1g} antiferroelectric rotation of the $Cr(CN)_6^{3-}$ octahedron, are the driving force of the phase transformations. The lattice instability in $Cs_2LiCr(CN)_6$ is similar in nature to the cell doubling transitions in $MTiO_3$ ($M = Ba^{2+}$, Sr^{2+}) where the titanate's distortions have been described as rotations of the TiO_6 octahedra with respect to the counterions (*1*).

Raman spectra taken as a function of temperature indicate that $Cs_2LiM(CN)_6$ ($M = Fe^{3+}$, Co^{3+}, Ir^{3+}) also undergo phase transformations (*6*). A correlation between the transition temperature and the cesium site size in the $Cs_2LiM(CN)_6$ salts shows that the transition temperature increases with the size of M. A similar correlation has been made for the rare earth aluminates $MAlO_3$ ($M = La^{3+}$, Pr^{3+}, Nd^{3+}, and Sm^{3+}) where a decrease in the size

ISSN 0022-4596

of the rare earth ion increases the transition temperature (*7*). The relationship between these two transitions can be easily visualized. The Cs^+ is analogous to the rare earth ion in that it fits into a tetrahedral hole defined by the metal–ligand–metal superlattice. Therefore, increasing the hole size in the trivalent hexacyanides is similar to decreasing the size of the rare earth in the perovskites.

This report is concerned with the lattice instabilities in the $Cs_2MFe(CN)_6$ ($M = Mg^{2+}$, Ca^{2+}, and Sr^{2+}) salts. The site size of the cesium in these ferrocyanides is determined by the size of the alkaline-earth counterion rather than by the transition metal in the hexacyanide moiety as is the case for the dicesium lithium salts. The crystal structure of the barium complex was solved with the hope that it would further clarify the previously proposed model for the distortions in $Cs_2LiCr(CN)_6$ (*2*).

Experimental Section

Crystals of $Cs_2CaFe(CN)_6$ and $Cs_2SrFe(CN)_6$ were grown by slow diffusion of $Cs_4Fe(CN)_6$ and the corresponding alkali chloride in a CsCl-doped water solution. The tetracesium salt was synthesized from $K_4Fe(CN)_6$ by ion exchange with Cs^+-replaced hydrogen from resin (Bio-Rad AG 50W-X16). The diffusion apparatus consisted of two test tubes bridged by 7-mm tubing fitted with two septum caps. Approximately 0.1 g of $Cs_4Fe(CN)_6$ and the alkali chloride were added to the assembly after it had been filled with a 0.1 *M* CsCl solution. With the septum caps securely fastened, the solution was thermostated at 35°C. The yellow crystals were harvested between 4 and 6 weeks later. Both of these salts are twinned and have nearly cubic habits. The largest Ca^{2+} and Sr^{2+} crystals had edges of 0.1 and 0.6 mm, respectively. The anhydrous forms of the Mg^{+2} (*8*), Ca^{2+} (*9*), and Sr^{2+} (*10*) salts have been prepared by similar methods. $Cs_2BaFe(CN)_6 \cdot 2H_2O$ was prepared by evaporation of a water solution containing CsCl, $Cs_4Fe(CN)_6$, and $BaCl_2$. The average size of the crystals was ca. 0.2 to 0.3 mm on an edge.

The Raman spectra of the Ca^{2+}, Sr^{2+}, and Ba^{2+} salts were gathered with a Cary 82 using the 5682 and 6472 Å lines of a Kr^+ ion laser (Spectra Physics 164).

The high-temperature phase transformation of the strontium salt was studied by Raman and optical methods. Raman spectra were recorded at various temperatures of a crystal mounted on a glass fiber. The sample was heated by a stream of hot nitrogen and its temperature was monitored by a thermocouple positioned 2 mm away from the crystal. $Cs_2SrFe(CN)_6$ crystals were also examined as a function of temperature with a Zeiss polarizing microscope. The temperature was was controlled by a Mettler FP2 microthermal apparatus.

A single crystal of $Cs_2BaFe(CN)_6 \cdot 2H_2O$ approximately 200 μm on an edge was mounted inside a glass capillary in the mother liquor. This was necessary since the crystal shattered when attempts were made to glue the crystals to a fiber. The crystal was mounted on a Syntex $P2_1$, computer-controlled, four-circle diffractometer equipped with a graphite-crystal incident beam monochromator. A least-squares refinement of 15 centered reflections produced the orientation matrix for data collection and gave cell constants of $a = 8.799(3)$, $b = 7.555(3)$, and $c = 11.607(5)$ Å and $\beta = 78.56(2)$ A°.

Data were collected in the range $0 < 2\theta > 50°$ using Mo$K\alpha$ $\lambda = 0.71069$ Å radiation. The θ–2θ scan technique with variable scan rate of 2.0 to 9.0°/min was used. The scan range was 2° in 2θ. Additional details of the method of data collection have been described previously. (*11*).

In order to check the stability of the X-ray measurements, three reflections were selected as standards and their intensities were measured periodically throughout data collection. No significant change was observed in these intensities. Of the 1610 reflections which were collected, 631 met the criterion $I \geq 3\sigma$. The data were corrected for Lorentz and polarization effects and an absorption correction was applied with ORABS which accounts for crystal shape (*12*). ORABS is a modified version of Busing and Levy's original program (*13*).

The heavy atom positions obtained from a

TABLE I

POSITIONAL AND THERMAL PARAMETERS FOR $Cs_2BaFe(CN)_6 \cdot 2H_2O$

Atom	x	y	z	μ_{11}[a]	μ_{22}	μ_{33}	μ_{12}	μ_{13}	μ_{23}
Ba	0.0	0.0	0.5	17(1)	24(1)	19(1)	0(6)	−6(1)	9(5)
Fe	0.0	0.0	0.0	15(1)	24(1)	17(1)	−16(5)	−4(1)	−14(4)
Cs	0.9198(1)	0.4811(10)	0.2096(1)	38(1)	14(3)	35(1)	−0.4(6)	−7(1)	0.6(5)
C_1	−0.0134(21)	0.0505(29)	0.1599(14)	29(8)	65(1)	14(7)	7(9)	7(6)	−4(7)
N_1	−0.0256(19)	0.916(23)	0.2589(15)	28(8)	29(1)	42(9)	−9(7)	−18(7)	5(7)
C_2	0.3716(30)	0.3054(33)	0.4849(21)	58(3)	29(2)	20(1)	18(1)	−6(9)	−6(9)
N_2	0.2939(20)	0.1788(21)	0.4705(14)	39(8)	14(8)	31(8)	−14(7)	0.3(7)	−5(6)
C_3	0.6789(26)	0.355(29)	0.4689(19)	36(2)	14(8)	19(9)	9(8)	−9(9)	5(8)
N_3	0.7946(21)	0.2725(29)	0.449(14)	37(8)	54(3)	23(8)	21(9)	3(6)	1(8)
O	0.2912(36)	0.3039(52)	0.1847(27)	99(1)	133(7)	157(9)	−92(1)	18(1)	−39(5)

[a] The mean-squared amplitudes have been multiplied by a factor of 10^3.

Patterson map provided a model for full-matrix least-squares refinements in the $P2_1/n$ space group. The function minimized was $\sum w^2(|F_0| - |F_c|)^2$, where w^2 is $1/\sigma^2(F_0)$. Neutral scattering factors (*14*) were used and anomolous dispersion corrections (*15*) were made for all atoms. The thermal motions were refined anisotropically and a secondary extinction correction was applied (*16*). The final R values were $R = 4.23\%$ and $R_w = 4.89\%$ where $R = \sum(|F_0| - |F_c|)/\sum|F_0|$ and $R_w = \sum w(|F_0| - |F_c|)/\sum w|F_0|$. Final difference Fourier maps show a maximum of 1.7 $e/Å^3$ in the vicinity of the metals but do not reveal any significant electron density around the carbon, nitrogen, and oxygen positions. The refined value of the secondary extinction coefficient is 4.6 (4) $\times 10^{-6}$. Final positional and thermal parameters are listed in Table I.

Discussion

Raman Spectra

In view of the structural similarities between the $Cs_2MFe(CN)_6$ ($M = Mg^{2+}$, Ca^{2+}, Sr^{2+}, and Ba^{2+}) and $Cs_2LiCr(CN)_6$ salts it is useful to consider the lattice instability and Raman spectra of the chromihexacyanide salt (*3*, *8–10*). The temperature-dependent Raman spectra of the chromihexacyanide salt show that the distortion can be described by lattice modes involving a rotation of the $Cr(CN)_6^{3-}$ octahedron and a translation of the Cs^+ (*2*). Above 348°K the spectra strictly follow the high-symmetry $Fm3m$ selection rules, and only the F_{2g} C–Cr–C deformation and the F_{2g} Cs–N stretch are observed below 200 cm^{-1}. As the temperature is decreased to 298°K, two new features appear at 30 and 100 cm^{-1}. These have been assigned, respectively, to a Cs^+ translation and a rotation of the hexacyanide moiety. Below room temperature the F_{1u} Cs^+ translational soft mode emerges from the exciting line while the lower site symmetry of the noncubic phase splits the F_{2g} C–Cr–C deformation mode into three bands. Finally, at 20°K all of the former F_{2g} and F_{1u} modes in the low-energy region are split into three components by the site symmetry.

The lattice instability in $Cs_2LiCr(CN)_6$ derives from the Cs^+ ion occupying a site which is too large. If the size of the cesium site is related to the transition temperature for the $Cs_2MFe(CN)_6$ salts, then an increase in the alkaline earth size should drive the transition temperature up. Accordingly, the room temperature spectra of the $Cs_2MFe(CN)_6$ complexes in going from Mg^{2+} to Ba^{2+} should be qualitatively similar to the spectra of $Cs_2LiCr(CN)_6$ obtained as a function of lowering the temperature. Thus, at a given temperature the amount of distortion from the parent $Fm3m$ structure should increase in proceeding from Mg^{2+} to Ba^{2+}.

The room temperature Raman spectra (see Fig. 1 and Table II) clearly indicate that the

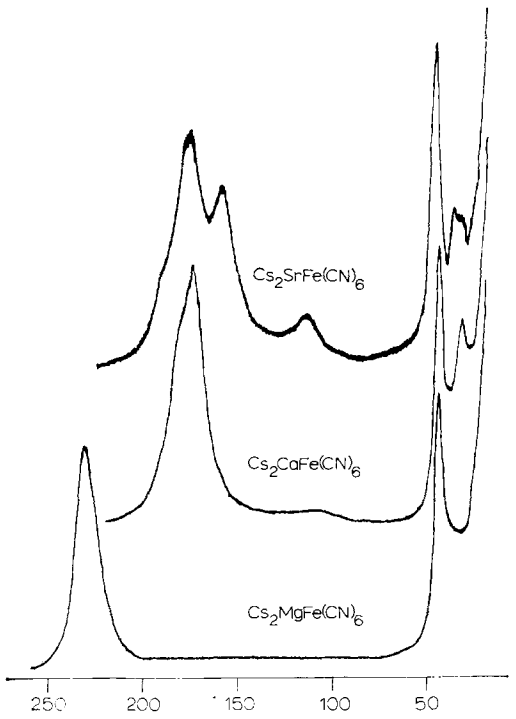

FIG. 1. The room temperature Raman spectra of $Cs_2MgFe(CN)_6$, $Cs_2CaFe(CN)_6$, and $Cs_2SrFe(CN)_6$. Units are in cm^{-1}.

distortion from the *Fm3m* phase increases going down the alkaline earths. The magnesium salt possesses the parent *Fm3m* (*8*) symmetry and its spectra follow cubic selection rules. However, from the spectra of $Cs_2CaFe(CN)_6$ it is apparent that the Ca^{2+} complex has undergone some distortion. The new features at ca. 109 and 30 cm^{-1} are markedly similar to the F_{1g} rotary mode and Cs^+ translational mode found in the chromihexacyanide salt. The shoulder on the C–Fe–C deformation also shows signs of mimicking the $Cs_2LiCr(CN)_6$ salt's behavior.

The similarities of the room-temperature spectra of $Cs_2SrFe(CN)_6$ and the low-temperature spectra of $Cs_2LiCr(CN)_6$ are even more striking. Besides a more intense rotary mode at 113 cm^{-1}, the C–Fe–C is split into two bands and there are now two additional bands in the Cs–N stretch region which can be attributed to Cs^+ translations.

The structure of the strontium salt was investigated as a function of temperature by Raman and optical methods. The large size of the crystals made the analysis by Raman spectroscopy possible. The spectra indicate that the phase change to cubic symmetry occurs at ca. 538°K. As the temperature was increased, the peaks in the C–Fe–C deformation region coalesced into one band and the lattice modes disappeared. The rotary mode diminished in intensity while the lower frequency Cs^+ translational mode merged with the exciting line. These results are supported by optical polarization experiments which show that the strontium crystals become isotropic at ca. 523°K.

The quality of the spectra for $Cs_2BaFe(CN)_6 \cdot 2H_2O$ is not as good as it is for the other salts. Even though this hampers comparisons, the spectra suggest even greater distortions. This is the only salt which shows a splitting in one of its CN stretch modes. Because of the presence of water and the quality of the spectra, the assignments for the low-energy region cannot be made with absolute confidence. There are six peaks below 120 cm^{-1}. Two of them can be readily assigned to a rotary mode, 113 cm^{-1}, and an F_{2g} Cs–N stretch, 42 cm^{-1}. The rest of the bands may arise from the splitting of these modes, barium–water lattice movements, or an F_{1u} Cs^+ translation.

The trend to larger distortions in going down the series is supported by the presence of an F_{1g} Fe–C–N deformation. All of the divalent hexacyanides except the magnesium salt have a band at ca. 347 cm^{-1}. F_{1g} metal cyanide deformations have been found between 300 and 350 cm^{-1} for $Cd_3[Co(CN)_6]_2 \cdot H_2O$ (*18*) and $Cs_2LiFe(CN)_6$ (*19*). This mode arises when the site symmetry of the transition metal is lowered, and its intensity increases with increasing distortion from cubic symmetry. In the barium complex this band is almost as intense as the Fe–C stretch mode whereas in the other two salts it is relatively much weaker.

For these hexacyanides and other structurally related salts, Raman spectroscopy provides a sensitive probe of small distortions which supplements X-ray crystallographic data. In a study of the phase transformation of $SrTiO_3$, Fleury *et al.* (*20*) noted that X-ray methods were insensitive to rotations of the TiO_6 octahedra since the displaced oxygen's

TABLE II

OBSERVED RAMAN MODES (cm^{-1})

Assignments[a]	$Cs_2MgFe(CN)_6$[b]	$Cs_2CaFe(CN)_6$	$Cs_2SrFe(CN)_6$	$Cs_2BaFe(CN)_6 \cdot 2H_2O$
ν_1 (A_{1g}, CN str)	2129.6	2120.7	2109.0	2097.7
ν_3 (E_g, CN str)	2090.6	2079.5	2068.5	2064.6
				2057.6
ν_{10} (F_{2g}, FeCN δ)	512.2	509.5	507.5	507.1
ν_4 (E_g, FeC str)				421.8 sh[d]
	437.0[c]	449.3[c]	434.9[c]	
ν_2 (A_{1g}, FeC str)				410.0
ν_5 (F_{1g}, FeCN δ)		345.0 vw[d]	346.9 vw	350.7
ν_{11} (F_{2g}, CFeC δ)	230.7	181.2 sh	188.1 sh	185.6 sh
		174.6	174.5	175.1
			158.8	151.1
ν_{14} (F_{1g}, rotatory)		108.7	113.4	113.1
Unassigned				89.2
				84.5
				65.3 vw
				54.9 vw
ν_{17} (F_{2g}, CsN str)	43.0	42.1	43.8	41.8
ν_{16} (F_{1u}, CsN str)		30.0	34.3	
			31.6	

[a] These are the symmetry species for the parent complex $Cs_2MgFe(CN)_6$. The frequencies of the other salts are listed according to their progenitors in the parent compound.

[b] Taken from Ref. (*17*).

[c] Unresolved ν_2 and ν_4.

[d] sh = shoulder, vw = very weak.

scattering factors are much smaller than those of Sr and Ti. Similarly, small rotations of hexacyanide moieties are difficult to detect by X-ray techniques. The incorrect space group assignment for $Cs_2CaFe(CN)_6$ illustrates this point. It had been indexed as cubic from a powder pattern (*9*), but its Raman spectra (see Fig. 1) clearly show deviations from the cubic selection rules of $Cs_2MgFe(CN)_6$.

The Crystal Structure of $Cs_2BaFe(CN)_6 \cdot 2H_2O$

Inspection of the distances and angles (see Table III) involving the ferrocyanide moiety reveals that it has maintained its octahedral symmetry. The Fe-C distances of 1.87(2), 1.88(3), and 1.89(2) Å agree favourably with the value of the iron carbon distance in $Cs_2MgFe(CN)_6$ (*8*), but the C–N distances of 1.17(2), 1.20(3), and 1.18(3) Å are longer than the expected 1.15 Å (*21*). Nevertheless, the C–N distances agree with the normal value within experimental error. The C–Fe–C and Fe–C–N angles are smaller than 90 and 180°, respectively. However, these idealized octahedral angles fall within the error ranges of the calculated angles. The environment of the ferrocyanide ion is depicted in Fig. 2.

Barium is 8-coordinate in the $Cs_2BaFe(CN)_6 \cdot 2H_2O$ lattice. Its nearly cubic coordination polyhedron is formed by six nitrogen- and two oxygens. The Ba–N distances are 2.93(2), 2.88(2), and 2.88(2) Å, while the Ba–O distance is 2.93(3) Å. All of the Ba–N–C angles fall around 150°.

The Cs^+ ion fits into an interstitial hole defined by the Fe–C–N–Ba framework, and it is surrounded by 12 CN^- moieties. The bond distances between the Cs^+ and the cyanides can be divided into two groups. The first consists of a set of three cyanides whose bond distances vary from 3.05 to 3.47 Å. The second group of distances range from 3.40 to 3.70 Å. The shortest Cs–N distance, 3.05 Å, is smaller than the sum of the Slater ionic radii for Cs^+

TABLE III

BOND DISTANCES AND ANGLES FOR $Cs_2BaFe(CN)_6 \cdot 2H_2O$

Atoms	Distance (Å)	Atoms	Distance (Å)	Atoms	Angle(°)
$Ba-N_1$	2.93(2)	$Cs-C_1$	3.33(2)	N_1-Ba-N_2	90.8(5)
$Ba-N_2$	2.88(2)		3.63(2)	N_1-Ba-N_3	57.6(5)
$Ba-N_3$	2.88(2)	$Cs-C_2$	3.47(2)	N_2-Ba-N_3	76.9(6)
Ba-O	2.93(3)		3.58(3)	C_2-Fe-C_1	89.3(9)
$Fe-C_1$	1.87(2)	$Cs-C_3$	3.44(3)	C_1-Fe-C_3	87.5(9)
$Fe-C_2$	1.88(3)		3.70(2)	C_2-Fe-C_3	88.7(12)
$Fe-C_3$	1.89(2)	$Cs-N_1$	3.05(2)	N_1-Ba-O	114.9(6)
C_1-N_1	1.17(2)		3.51(2)	N_2-Ba-O	105.5(9)
C_2-N_2	1.20(3)	$Cs-N_2$	3.29(2)	N_3-Ba-O	122.7(6)
C_3-N_3	1.18(3)		3.40(2)	$F-C_1-N_1$	176(2)
		$Cs-N_3$	3.19(2)	$Fe-C_2-N_2$	177(2)
			3.62(2)	$Fe-C_3-N_3$	177(2)
		Cs-O	3.49(4)	$Ba-N_1-C_1$	149(2)
				$Ba-N_2-C_2$	151(2)
				$Ba-N_3-C_3$	153(2)

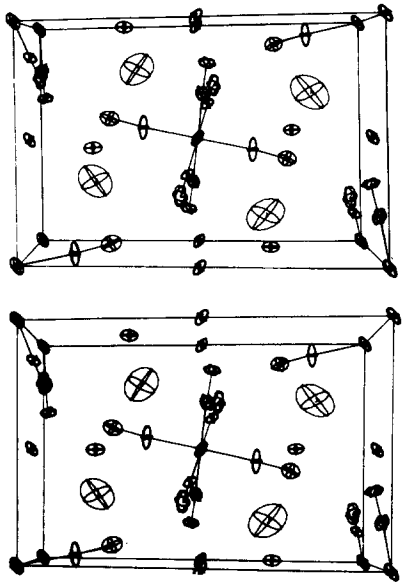

FIG. 2. A stereographic view of $Fe(CN)_6^{4-}$ in the $Cs_2BaFe(CN)_6 \cdot 2H_2O$ lattice. The ferrohexacyanide moiety is shown as a unit. The large ellipsoids in the center of the cell are water molecules. Six barium atoms are located in the faces or on the edges of the cell while each of the four cesium atoms are in the proximity of a water molecule.

and CN^-. In contrast to the cubic $Cs_2LiM(CN)_6$ salts and $Cs_2MgFe(CN)_6$, this complex has a substantial pairwise interaction between these two species.

Lattice Instabilities

In the $Cs_2LiM(CN)_6$ complexes a correlation exists between the cesium site size and the lattice instabilities (*2*, *6*). As the cesium hole size increases in going from the Co^{3+} to the Cr^{3+} salt, the cubic lattice becomes more unstable with respect to distortion. By varying the transition metal, the cesium site size can be altered without dramatically changing the interionic potentials or the mass of the complex ion. This simplicity is lost in going down the $Cs_2MFe(CN)_6$ series where both the *M*–N potentials and the mass of *M* change. Nevertheless, the Raman data suggest that the lattice instability increases monotonically as the size of *M* is increased. Apparently, the primary factor influencing the instability is the size of the cesium hole.

A direct comparison of the lattice instabilities in the barium salt and $Cs_2LiCr(CN)_6$ is complicated by the presence of water. It is improbable that the dihydrate would undergo phase transformations similar to those observed in $Cs_2LiCr(CN)_6$. Nevertheless, the barium structure closely models the $P2_1/n$ monoclinic phase of $Cs_2LiCr(CN)_6$. (*2*) Surprisingly, the structure can be described in terms of phonons for a parent *Fm3m* cubic cell. This cubic cell is merely a construct for comparative purposes since the complex would decompose before it reached the cubic

phase. Like the chromium salt, the distortions involve a rotation of the $Fe(CN)_6^{4-}$ moiety and a translation of the Cs^+.

At room temperature $Cs_2BaFe(CN)_6 \cdot 2H_2O$ is much further below its transition temperature than $Cs_2LiCr(CN)_6$ is below its own transition temperature. As a result, the Ba^{2+} salt's distortions are more pronounced. In $Cs_2LiCr(CN)_6$ the chromihexacyanide moiety rotates 6° about the z axis and Cs^+ translates 0.09 Å along the y direction, whereas in the barium complex the rotation of the $Fe(CN)_6^{4-}$ ion is much greater (as evidenced by the ca. 150° Ba–N–C angles) and the Cs^+ moves approximately 0.4 Å in each of the x, y, and z directions. Even though the $P2_1/n$ space group allows other degrees of freedom (rotation about x and y and Cs^+ translation along x and z) the $Cr(CN)_6^{3-}$ ion only rotates about one axis and the Cs^+ moves only in one direction. In the $Cs_2BaFe(CN)_6 \cdot 2H_2O$ salt distortions occur along all of the symmetry allowed phonon directions. It is likely that $Cs_2LiCr(CN)_6$ distorts along these four additional degrees of freedom below room temperature.

A comparison of the cesium temperature factors in the $Cs_2BaFe(CN)_6 \cdot 2H_2O$ and $Cs_2LiM(CN)_6$ (*3*, *4*, *22*) structures adds to our picture of the instability. The cesium motion in the barium salt is reasonable, whereas in the cubic hexacyanides it is abnormally large. The large hole size of the cubic structures results in a weak cesium–cyanide interaction and a high cesium thermal motion. In $Cs_2BaFe(CN)_6 \cdot 2H_2O$ the shorter bond between the cesium and cyanide moieties reduces the cesium motion. Thus, the greater stability of the lower-symmetry phase with respect to the cubic phase is reflected in this decrease in the cesium thermal motion.

Acknowledgments

This work was supported by the Robert A. Welch Foundation (Grant No. F-620). We would also like to thank Bonnie Lucas for help in obtaining the optical measurements.

Note added in proof. The table of structure factors has been deposited as NAPS Document No. 02986 (7 pages).

References

1. J. F. Scott, *Rev. Mod. Phys.* **46**, 83 (1974).
2. R. R. Ryan and B. I. Swanson, *Phys. Rev. B* **13**, 5320 (1976).
3. R. R. Ryan and B. I. Swanson, *Inorg. Chem.* **13**, 1681 (1974).
4. J. R. Armstrong, B. M. Chadwick, D. W. Jones, J. E. Sarneski, H. J. Wilde, and J. Yerkess, *Inorg. Nucl. Chem. Lett.* **9**, 1025 (1973).
5. J. C. Slater, *J. Chem. Phys.* **41**, 3199 (1964).
6. B. I. Swanson and B. C. Lucas, unpublished results.
7. J. F. Scott and J. P. Remeika, *Phys. Rev. B*, **1**, 4182 (1970).
8. B. I. Swanson, S. I. Hamburg, and R. R. Ryan, *Inorg. Chem.* **13**, 1685 (1974).
9. V. G. Kuznetsov, Z. V. Popova, and G. B. Seifer, *Russ. J. Inorg. Chem.* (English Transl.) **15**, 1250 (1970).
10. V. G. Kuznetsov, Z. V. Popova, and G. B. Seifer, *Russ. J. Inorg. Chem.* **15**, 1084 (1970).
11. F. A. Cotton, B. A. Frenz, G. D. Deganello, and A. Shaver, *J. Organometal. Chem.* **50**, 227 (1973).
12. This modified version of Busing and Levy's program was written by R. E. Davis.
13. W. R. Busing and H. A. Levy, *Acta Crystallogr.* **10**, 180 (1957).
14. D. T. Cromer and J. B. Mann, *Acta Crystallogr. Sect. A* **24**, 321, (1968).
15. D. T. Cromer, *Acta Crystallogr.* **18**, 17 (1965).
16. A. C. Larson, *Acta Crystallogr.* **23**, 664 (1967).
17. B. I. Swanson and J. J. Rafalko, *Inorg. Chem.* **15**, 249 (1976).
18. B. I. Swanson, *Inorg. Chem.* **15**, 253 (1976).
19. B. I. Swanson, B. C. Lucas, and R. R. Ryan, unpublished results.
20. P. A. Fleury, J. F. Scott, and J. M. Worlock, *Phys. Rev. Lett.* **21**, 16 (1968).
21. A. G. Sharpe, "The Chemistry of Cyano Complexes of the Transition Metals," Academic Press, New York, 1976.
22. B. I. Swanson and R. R. Ryan, *Inorg. Chem.* **12**, 283 (1973).